Peroxidase evolution in white-rot fungi follows wood lignin evolution in plants

Iván Ayuso-Fernández[a], Jorge Rencoret[b], Ana Gutiérrez[b], Francisco Javier Ruiz-Dueñas[a], and Angel T. Martínez[a,1]

[a]Centro de Investigaciones Biológicas, Consejo Superior de Investigaciones Científicas, E-28040 Madrid, Spain; and [b]Instituto de Recursos Naturales y Agrobiología de Sevilla, Consejo Superior de Investigaciones Científicas E-41012 Seville, Spain

Edited by David M. Hillis, The University of Texas at Austin, Austin, TX, and approved July 25, 2019 (received for review March 23, 2019)

A comparison of sequenced Agaricomycotina genomes suggests that efficient degradation of wood lignin was associated with the appearance of secreted peroxidases with a solvent-exposed catalytic tryptophan. This hypothesis is experimentally demonstrated here by resurrecting ancestral fungal peroxidases, after sequence reconstruction from genomes of extant white-rot Polyporales, and evaluating their oxidative attack on the lignin polymer by state-of-the-art analytical techniques. Rapid stopped-flow estimation of the transient-state constants for the 2 successive one-electron transfers from lignin to the peroxide-activated enzyme (k_{2app} and k_{3app}) showed a progressive increase during peroxidase evolution (up to 50-fold higher values for the rate-limiting k_{3app}). The above agreed with 2-dimensional NMR analyses during steady-state treatments of hardwood lignin, showing that its degradation (estimated from the normalized aromatic signals of lignin units compared with a control) and syringyl-to-guaiacyl ratio increased with the enzyme evolutionary distance from the first peroxidase ancestor. More interestingly, the stopped-flow estimations of electron transfer rates also showed how the most recent peroxidase ancestors that already incorporated the exposed tryptophan into their molecular structure (as well as the extant lignin peroxidase) were comparatively more efficient at oxidizing hardwood (angiosperm) lignin, while the most ancestral "tryptophanless" enzymes were more efficient at abstracting electrons from softwood (conifer) lignin. A time calibration of the ancestry of Polyporales peroxidases localized the appearance of the first peroxidase with a solvent-exposed catalytic tryptophan to 194 ± 70 Mya, coincident with the diversification of angiosperm plants characterized by the appearance of dimethoxylated syringyl lignin units.

fungal evolution | lignin evolution | ancestral peroxidases | stopped-flow spectrophotometry | NMR spectroscopy

Lignin is an aromatic polymer formed by dehydrogenative coupling of *p*-hydroxycinnamyl alcohols and other phenols (1) that confers resistance and other properties to vascular plants. Due to lignin recalcitrance, its degradation is essential for carbon recycling in nature and often represents a limiting step for a biobased economy (2). The biological degradation of lignin is described as an enzymatic combustion (3) typically made by Polyporales and other white-rot Agaricomycetes. It involves the so-called manganese peroxidases (MnPs), versatile peroxidases (VPs), and lignin peroxidases (LiPs) together with auxiliary enzymes (4). MnPs oxidize the often minor phenolic moiety of lignin via Mn^{3+} chelates or directly at the heme cofactor (5). In contrast, LiPs attack nonphenolic lignin directly using a solvent-exposed catalytic tryptophan forming a reactive radical, as shown using model compounds (6). Finally, VPs combine the structural and catalytic properties of MnPs and LiPs (7), including the surface tryptophan, whose role in direct oxidation of lignin was recently demonstrated (8).

Fungal degradation of lignin via white rot arose around the Carboniferous period, associated with the production of the first ligninolytic peroxidases (9) and, along with geochemical factors, may have contributed to the decline of carbon sequestration (coal formation) toward the end of the Permo-Carboniferous period (10). Recent works have resurrected ancestral ligninolytic peroxidases and analyzed their evolution in Polyporales using high– and low–redox potential simple model substrates (11). These studies suggest that the most ancestral ligninolytic enzymes acted on phenolic lignin and later shaped their oxidation sites several times to become first VPs and later LiPs, the most efficient lignin-degrading enzymes, as a convergent trait in fungal evolution (12). Also, ligninolytic peroxidases progressively increased the redox potential of their reactive species (13). Finally, their stability at acidic pH, where lignin decay takes place in nature, increased, and their catalytic tryptophan environment became more negative to stabilize lignin cation radicals (11, 12).

Recent phylogenomic studies on over 1,000 Agaricomycetes suggest that during evolution wood-rotting fungi became host specific depending on whether they were brown-rot fungi, often acting on conifers, or white-rot fungi, specializing on angiosperms (14). The evolution of host specialization is notably interesting since conifer lignin basically consists of guaiacyl (G) units, while angiosperms introduce also syringyl (S) units, with minor amounts of *p*-hydroxyphenyl (H) units in both lignins, as illustrated in Fig. 1 (see *SI Appendix*, Table S1, for a comprehensive review of lignin composition). As shown in Fig. 1, S-type units were also incorporated by some nonconifer gymnosperms and a few ferns and lycophytes as an example of convergent evolution discussed below. Lignin in conifers did not show detectable changes during evolution (15). Then, the general inclusion of S units in angiosperms

Significance

We analyze the evolution of ligninolytic peroxidases from wood-rotting fungi using conifer and angiosperm lignin as representatives of 2 steps of lignin evolution. By enzyme resurrection, we show that during fungal evolution, these enzymes improved their activity and switched their degradative preferences with the rise of a surface tryptophan conferring on them the ability to oxidize nonphenolic lignin. We calibrated the peroxidase phylogeny and determined that this residue appeared coincident with angiosperm diversification, characterized by the synthesis of a more complex and less phenolic lignin due to the general incorporation of a new unit in its structure. This way, we show that fungal evolution followed that of lignin synthesis, pointing to a coevolution between fungal saprotrophs and their plant hosts.

Author contributions: F.J.R.-D. and A.T.M. designed research; I.A.-F. and J.R. performed research; A.G. contributed new reagents/analytic tools; I.A.-F., F.J.R.-D., and A.T.M. analyzed data; I.A.-F. performed bioinformatic analysis; and I.A.-F., F.J.R.-D., and A.T.M. wrote the paper.

The authors declare no conflict of interest.

This article is a PNAS Direct Submission.

[1]To whom correspondence may be addressed. Email: atmartinez@cib.csic.es.

This article contains supporting information online at www.pnas.org/lookup/suppl/doi:10.1073/pnas.1905040116/-/DCSupplemental.

Published online August 19, 2019.

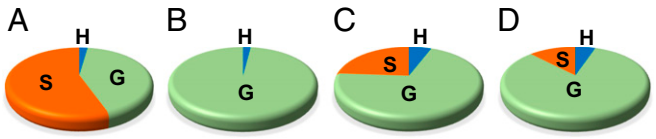

Fig. 1. Average lignin composition (H, G, and S molar content) in angiosperms (*A*), conifers (*B*), other gymnosperms (*C*), and ferns and lycophytes (*D*) from a total of 144 species (see *SI Appendix*, Table S1, for the complete inventory).

resulted in a more complex lignin providing mechanical and physiological advantages to plants (16, 17).

So far, the evolution of ancestral peroxidase has not been analyzed using the lignin polymer as a substrate since initial rates of lignin oxidation cannot be obtained under steady-state conditions. However, the electron transfer rates can be accurately estimated from the reduction of peroxide-activated enzymes by lignin under stopped-flow conditions (8, 18). Among available lignin preparations, lignosulfonates are unique because of their water solubility, a requisite for the above stopped-flow analyses. These preparations originate from sulfite pulping of wood, a process based on lignin sulfonation (19). While solubilizing lignin, sulfonation scarcely affects peroxidase reactivity (18). Here we investigate how ancestral peroxidases modify lignin through their evolution and estimate the electron transfer rates from softwood and hardwood lignosulfonates. With this purpose, we use stopped-flow rapid spectrophotometry to calculate transient-state kinetic parameters and 2-dimensional (2D) NMR spectroscopy to evaluate the polymer modification in extended steady-state treatments.

Results

Evolution of Polyporales Lignin-Degrading Peroxidases. To investigate how the ability to oxidize the lignin polymer evolved in the ancestry of Polyporales peroxidases (20), we reconstructed with PAML the lineage leading to the well-known isoenzyme H8 of *Phanerochaete chrysosporium* LiP, corresponding to gene A in the sequenced genome (PC-LiPA) (21). Then, we resurrected by *Escherichia coli* expression (11) the main nodes in the evolutionary

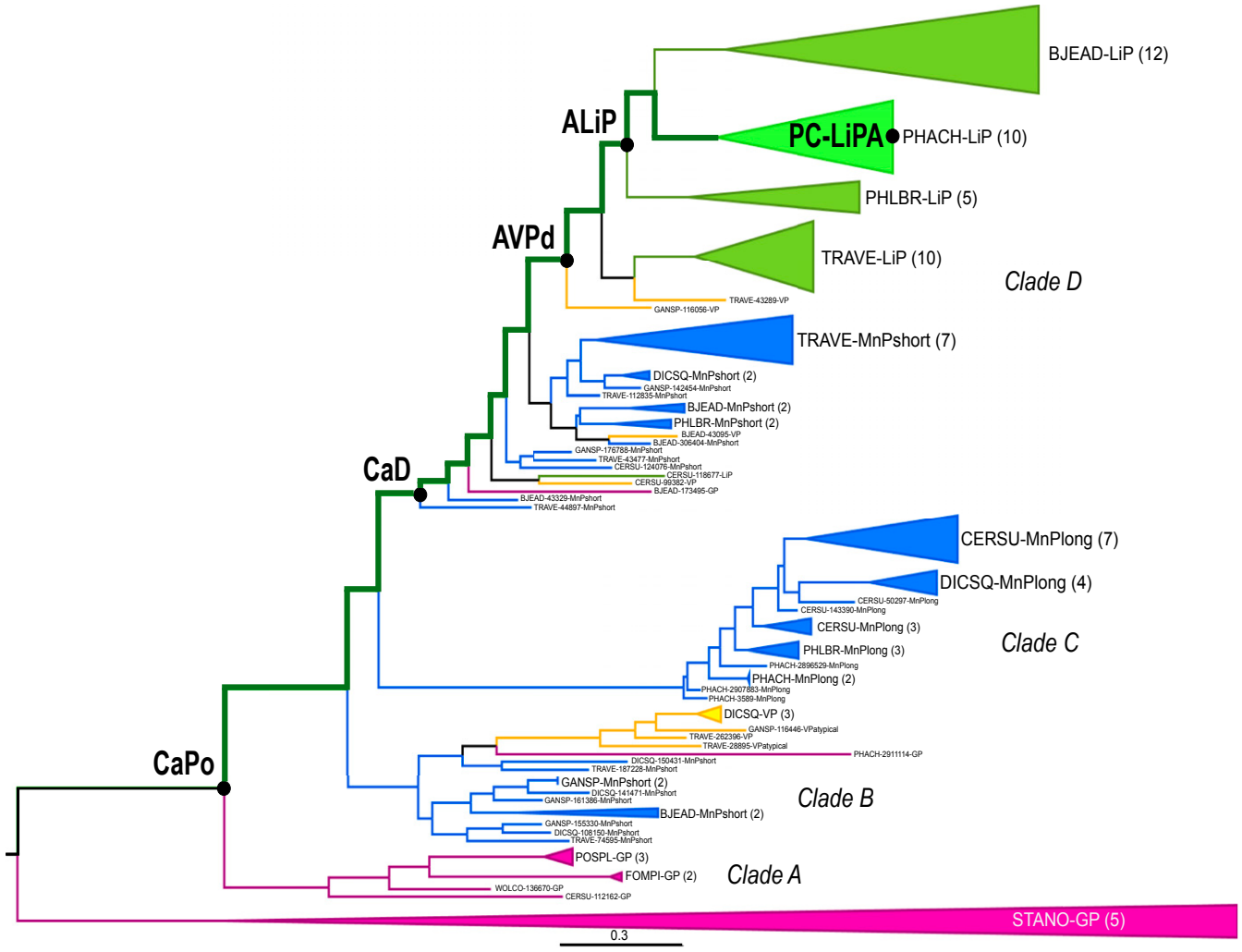

Fig. 2. Evolution of Polyporales peroxidases from 10 sequenced genomes (12), including the *Stagonospora nodorum* generic peroxidases (GPs) for rooting the tree built by RAxML. Collapsed clusters are shown in green (LiPs), yellow (VPs), blue (MnPs) and purple (GPs). The path to the extant PC-LiPA is marked in green, including CaPo (common ancestor of Polyporales peroxidases), CaD (common ancestor of clade D), AVPd (ancestral VP in clade D), and ALiP (ancestral LiP). Labels start with the species (BJEAD, *Bjerkandera adusta*; CERSU, *Ceriporiopsis subvermispora*; DICSQ, *Dichomitus squalens*; FOMPI, *Fomitopsis pinicola*; GANSP, *Ganoderma* sp.; PHLBR *Phlebia brevispora*; PHACH, *P. chrysosporium*; POSPL, *Postia placenta*; STANO, *S. nodorum*; TRAVE, *Trametes versicolor*; and WOLCO, *Wolfiporia cocos*), followed by the JGI ID and the peroxidase type (GP, LiP, MnP short, MnP long, VP, or VP atypical).

Table 1. Kinetic constants for CI/CII and CII/RS reduction in ancestral (CaPo, CaD, AVPd, and ALiP) and extant (PC-LiPA) peroxidases by softwood and hardwood lignosulfonate (LS)

Reduction	Lignin type	Constant	CaPo	CaD	AVPd	ALiP	PC-LiPA
CI/CII	Softwood LS	K_{D2} (μM)	46 ± 3	57 ± 3.9	46 ± 3.3	44 ± 15	23 ± 1
		k_2 (s^{-1})	9 ± 0	20 ± 1	19 ± 1	42 ± 9	33 ± 2
		k_{2app} ($s^{-1}·mM^{-1}$)	197 ± 14	351 ± 34	413 ± 33	955 ± 385	1,440 ± 120
	Hardwood LS	K_{D2} (μM)	—	—	8 ± 1	40 ± 5	8 ± 2
		k_2 (s^{-1})	—	—	18 ± 0.6	27 ± 1.4	25 ± 0.9
		k_{2app} ($s^{-1}·mM^{-1}$)	86 ± 18	202 ± 7	2,280 ± 280	674 ± 97	2,940 ± 740
CII/RS	Softwood LS	K_{D3} (μM)	—	—	102 ± 12	—	95 ± 326
		k_3 (s^{-1})	—	—	10 ± 1	—	25 ± 4
		k_{3app} ($s^{-1}·mM^{-1}$)	25 ± 8	78 ± 4	99 ± 14	331 ± 4	263 ± 83
	Hardwood LS	K_{D3} (μM)	—	—	9 ± 2	58 ± 8	19 ± 2
		k_3 (s^{-1})	—	—	6 ± 0	29 ± 1	14 ± 0
		K_{3app} ($s^{-1}·mM^{-1}$)	16 ± 3	43 ± 1	670 ± 145	500 ± 70	764 ± 86

Means and 95% confidence limits are from reactions at 25 °C in 0.1 M tartrate, with a pH of 3. A dash (—) indicates no saturation was reached. K_{D2} and K_{D3}, CI and CII dissociation constants; k_2 and k_3, CI and CII first-order rate constants; k_{2app}, CI apparent second-order rate constant.

line (Fig. 2) and characterized the degradative abilities of these ancestral enzymes using polymeric lignin as a substrate.

Previously, to calibrate the age of ancestral peroxidases in the RAxML tree in Fig. 2, we built an ultrametric tree with PATHd8, which uses mean path lengths from the leaves of a tree with a correction of the deviation from a molecular clock by smoothing substitution rates locally (*SI Appendix*, Fig. S1). The ages obtained suggest that the evolution of ligninolytic peroxidases started 399 ± 140 Mya with a common ancestor of Polyporales peroxidases (CaPo), which most likely was the ancestor of all Agaricomycetes class II peroxidases (9, 12). CaPo had a Mn^{2+}-binding site for oxidation of this metal cation but also oxidized phenolic substrates in direct contact with the heme (11). From CaPo, the lineage to extant LiPs did not experience significant changes for 200 million years (with the common ancestor of clade D peroxidases [CaD] dated to 259 ± 94 Mya still being a MnP-type enzyme) until the appearance of the catalytic tryptophan in ancestral VP in clade D (AVPd) 194 ± 70 Mya. AVPd retained the Mn^{2+} oxidation site together with the new solvent-exposed tryptophan, putatively responsible for nonphenolic lignin oxidation. Then, a quick change, losing the Mn^{2+}-binding site, occurred in a few million years, originating the first LiP of the phylogeny (ancestral LiP [ALiP], 178 ± 64 Mya) that further led to the extant LiPs maintaining the oxidation site architecture. This last evolutionary step resulted in a highly specialized enzyme whose efficient oxidation of nonphenolic lignin is not noncompetitively inhibited by Mn^{2+}, as in the case of VPs.

Kinetics of Lignin Oxidation through Peroxidase Evolution. For better biological understanding of peroxidase evolution, we analyzed the catalytic cycle of the resurrected ancestors with lignosulfonates as enzyme-reducing substrates. This cycle (18) includes 2-electron activation of the resting state (RS) enzyme by H_2O_2 forming compound I (CI), which is reduced back to RS via a 1-electron oxidized compound II (CII) yielding 2 product molecules (*SI Appendix*, Fig. S2). The different ultraviolet–visible spectra of these intermediates make following the cycle reactions by stopped-flow rapid spectrophotometry possible. The CI/CII and CII/RS reduction kinetic curves were obtained, and the corresponding transient-state constants for hardwood and softwood lignins were estimated (Table 1) with dissociation (K_D) and first-order rate (k) constants being calculated when the pseudo-first-order rate constant k_{obs} exhibited saturation behavior (as illustrated in Fig. 3 and *SI Appendix*, Fig. S3).

For all enzymes, CII/RS reduction is the rate-limiting step, with the most ancestral CaPo and CaD having significantly slower rates than the enzymes with the catalytic tryptophan (AVPd, ALiP, and PC-LiPA) (Fig. 4). For softwood lignin there is a progressive increase of the CII apparent second-order rate constant (k_{3app}) through evolution, but the differences between enzymes do not exceed a 13-fold increase. However, for hardwood lignin there is a huge boost in k_{3app}, increasing nearly 50-fold from CaPo to AVPd, when the solvent-exposed tryptophan appeared. These increments can be interpreted in terms of the dissociation constant (K_{D3}), indicating a greater affinity for the polymer in the enzymes with the solvent-exposed tryptophan (Fig. 3*B*). Therefore, a change in lignin preference was produced through peroxidase evolution: The ratio between hardwood and softwood lignosulfonate rate-limiting k_{3app} is less than 1 for the enzymes lacking the catalytic tryptophan and greater (up to 7) for those incorporating that residue.

Steady-State Treatment of Lignins. To further explore the evolution of lignin degradation, the structural modification of G and S–G lignins from softwood and hardwood, respectively, was analyzed by heteronuclear single quantum correlation (HSQC) 2D NMR spectroscopy. The signals of the main aromatic units and side chain interunit linkages in hardwood (Fig. 5) and softwood (*SI Appendix*, Fig. S4) lignosulfonates included Cα-sulfonated guaiacyl units (**G**) and Cα-sulfonated (**S**), nonsulfonated (***S***), and Cα-oxidized (**S′**) syringyl units, together with Cα-sulfonated (**A**) and nonsulfonated (***A***) β-*O*-4′ substructures and less abundant phenylcoumaran (***B***) and resinol (***C***) substructures. A semi-quantitative analysis of these signals provided the lignin decrease (from aromatic signals), referred to the control without enzyme, and S/G ratio and substructure composition referred to 100 aromatic units (*SI Appendix*, Table S2).

Twenty-four-hour treatments of softwood lignosulfonate with the ancestral enzymes and PC-LiPA did not reveal strong differences between them or from the enzyme-free control (*SI Appendix*, Fig. S4). However, the same treatments on hardwood lignosulfonate resulted in significant spectroscopic changes (Fig. 5 and *SI Appendix*, Table S2), a fact related to the peroxidase evolution acting on angiosperm lignin discussed below. By integrating the aromatic signals in the hardwood lignosulfonate spectra, we observed a decrease through evolution being the maximal change produced by ALiP (with a 59% decrease of S units and an 81% decrease of G units). This is accompanied by an overall increase (over 2-fold) of the S/G ratio. Concerning side chain signals, no strong changes in their relative abundance (per 100 aromatic units) were observed.

The progressive decrease of lignin signals in the steady-state treatments through peroxidase evolution supports the trend observed in stopped-flow measurements. Interestingly, in both

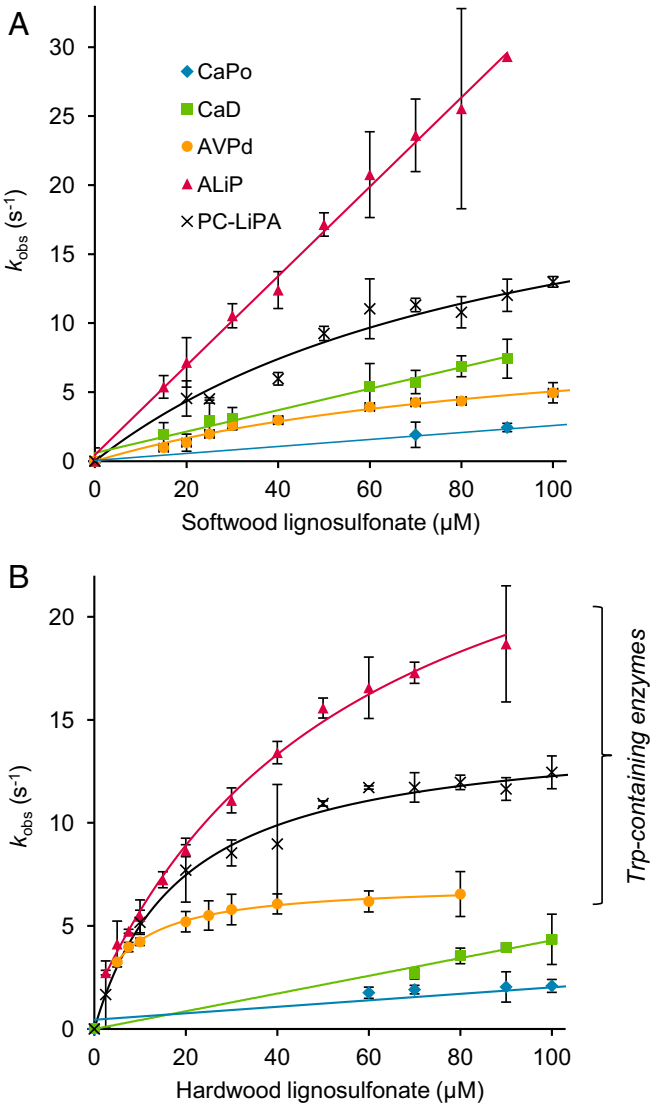

Fig. 3. Kinetics of CII to RS reduction in ancestral (CaPo, CaD, AVPd, and ALiP) and extant (PC-LiPA) peroxidases by softwood (*A*) and hardwood (*B*) lignosulfonates. The lignosulfonate concentrations refer to the basic phenylpropanoid unit. Means and 95% confidence limits are shown. More efficient enzymes containing a catalytic tryptophan residue are indicated in *B*.

cases, the strongest change coincided with the evolutionary appearance of the surface catalytic tryptophan.

Polyporales Specialization for Plant Substrates. Using the U.S. Department of Agriculture (USDA) Fungus-Host Distribution Database (https://nt.ars-grin.gov/fungaldatabases/fungushost/fungushost.cfm), we obtained a list of plant hosts for the 10 Polyporales species analyzed. This information was compared with the number and type of peroxidase genes in the genomes of the same fungi, extracted from the Joint Genome Institute (JGI) MycoCosm database (https://mycocosm.jgi.doe.gov/mycocosm/home) (*SI Appendix*, Table S3). With only the exception of *P. brevispora* (with only 3 citations), a correlation could be found between the specialization toward angiosperm decay and the number of peroxidases with the solvent-exposed catalytic tryptophan (VPs or LiPs). When the analysis was extended to the 64 Polyporales genomes currently available at JGI, the same tendency was observed, with surface tryptophan being present in 32% of the peroxidases from fungi with preference for angiosperm hosts versus only 15% in conifer-colonizing fungi (Fig. 6).

Discussion

Genomic studies from 2004 (21) demonstrated the presence of ligninolytic peroxidase (LiP, VP, and/or MnP) genes in all typical white-rot fungi sequenced (9, 20, 22), although some controversy has been raised regarding a few poor wood degraders (23). More recently, several aspects of peroxidase evolution were addressed by ancestral sequence reconstruction and characterization of the resurrected ancestors using simple substrates (11–13). Here, we use softwood and hardwood lignin as substrates to analyze the evolution leading to the most efficient ligninolytic enzymes, Polyporales LiPs (4).

With both types of lignin, the efficiency of the rate-limiting electron transfer step (corresponding to CII reduction to RS) was higher for the enzymes containing the catalytic tryptophan (AVPd, ALiP, and PC-LiPA). This is in agreement with the decreased electron transfer rate observed for tryptophanless variants of extant VP (18). As shown by stopped-flow spectrophotometry, uniquely interesting is the change in specificity when the solvent-exposed tryptophan appeared in AVPd. These analyses reveal a switch from better oxidation of softwood lignin by the oldest CaPo and CaD ancestors (although with low kinetic rates on both lignins) to better oxidation of hardwood lignin since then (by AVPd, ALiP, and PC-LiPA enzymes). Moreover, using state-of-the-art 2D NMR (24), enzymatic modification of lignin was observed in steady-state treatments of lignosulfonates with the peroxidase ancestors. Especially informative are the results from hardwood lignosulfonates, revealing that the lignin-degrading ability increases as a result of evolution being higher in the enzymes containing the solvent-exposed catalytic tryptophan, in agreement with the stopped-flow measurements.

During recent evolution of vascular plants, the route to S units appeared before the diversification of angiosperms, which started 250 to 140 Mya (25), and remains present in all extant species (*SI Appendix*, Table S1). The presence of S-type lignin in some nonangiosperm plants (*SI Appendix*, Table S1, including reports of S content >25% for 1 liverwort, 3 lycophytes, 1 fern, and 3 gnetophyte lignins) most likely represents evolutionary convergence events (26), as demonstrated for the lycophyte *Selaginella*

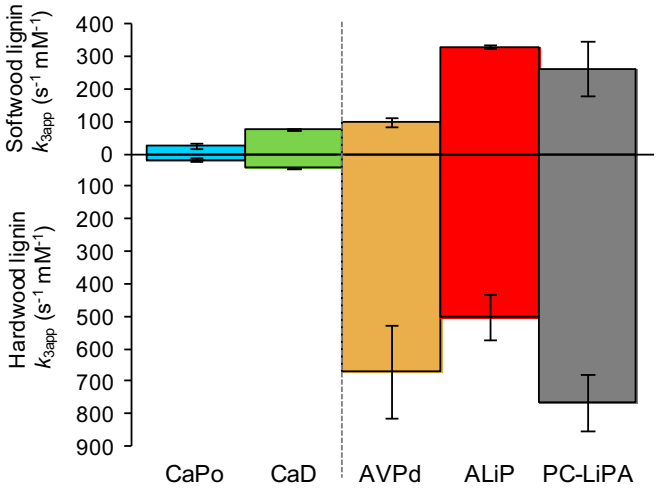

Fig. 4. Comparison of the rate-limiting step constant (k_{3app}) in lignin stopped-flow transient-state kinetic experiments with ancestral and extant peroxidases, showing a shift from softwood to hardwood lignin preference with the appearance of the catalytic tryptophan in AVPd (dashed line). Means and 95% confidence limits are shown.

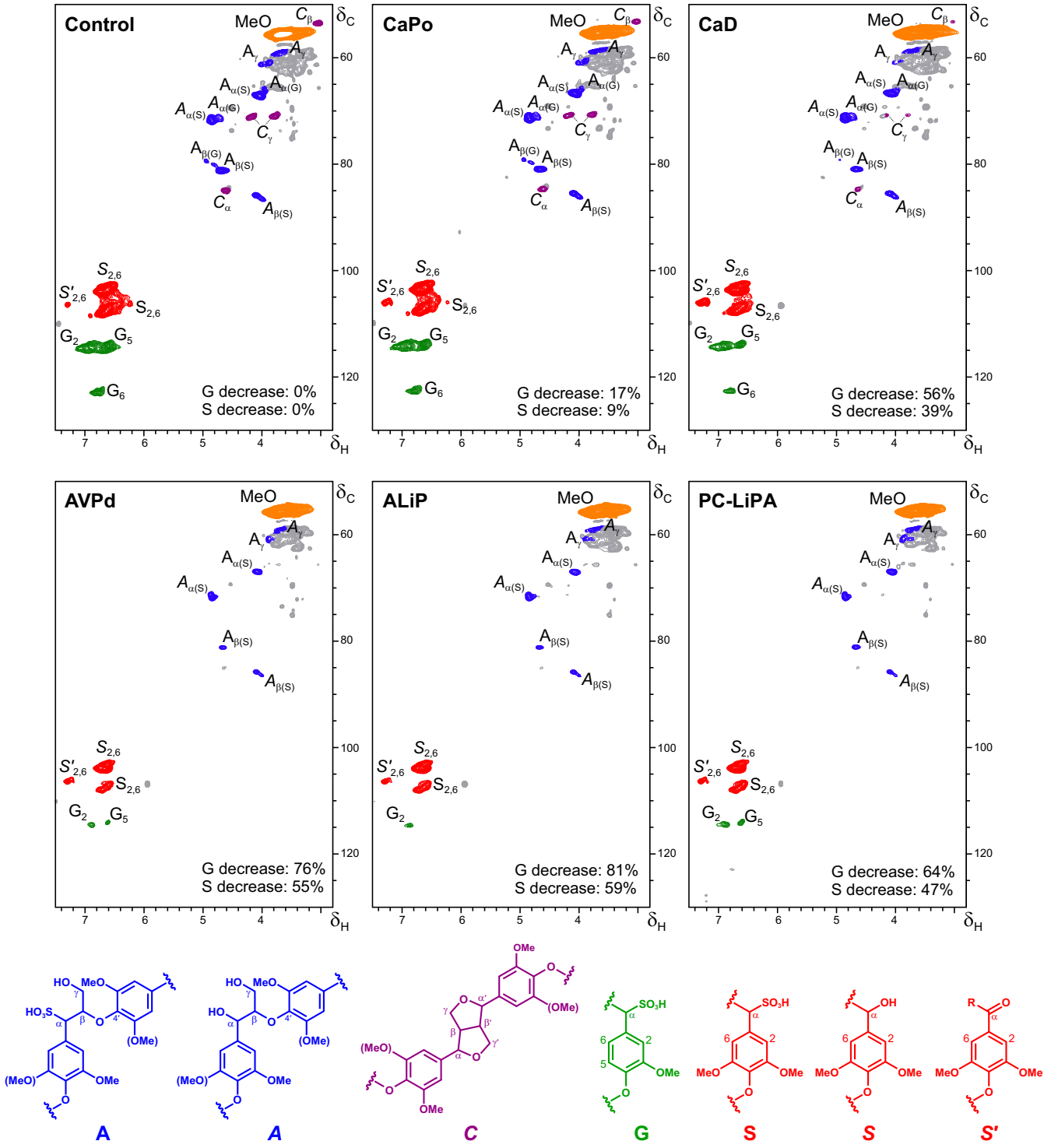

Fig. 5. HSQC NMR spectra of hardwood lignosulfonate treated for 24 h with ancestral peroxidases and extant PC-LiPA, and control without enzyme. The main substructures identified are included at the bottom, and the decrease in G and S units (with respect to the control) are indicated in each panel. Signals correspond to $^{1}H–^{13}C$ correlations at the different positions of Cα-sulfonated guaiacyl units (**G**); Cα-sulfonated, nonsulfonated, and Cα-oxidized syringyl units (**S**, ***S***, and **S′**); Cα-sulfonated and nonsulfonated β-*O*-4′ substructures (**A** and ***A***) and resinol (***C***) substructures; and methoxyls (MeO).

moellendorffii (27). In a broader context, it has been suggested that S units emerged at least 5 times during plant evolution, including "lignin-like" molecules in some nonvascular plants (28), although a stable and generalized presence was only produced in flowering plants. Wood lignin containing S units has higher complexity (1) and lower phenolic content (29, 30), reducing enzymatic degradability. Due to the apparent implication of the surface tryptophan mentioned above in the oxidation of nonphenolic lignin, we calibrated here its evolutionary appearance. This time calibration suggests that AVPd, the first ancestral peroxidase with this exposed tryptophan, appeared 194 ± 70 Mya, concurrent with angiosperm diversification.

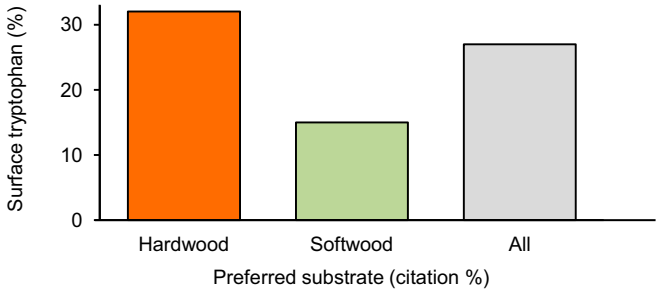

Fig. 6. Hardwood and softwood preference of Polyporales vs. the frequency of the catalytic surface tryptophan in peroxidases. The percentage of peroxidases with the surface catalytic tryptophan is from a survey of genes (up to a total of 794) in 64 genomes sequenced at JGI. The substrate preference was defined from the number of angiosperm and conifer hosts included in the USDA Fungus-Host Distribution Database.

Our results show how saprotrophic fungi followed lignin evolution in plants incorporating a catalytic tryptophan responsible for oxidation of the more complex and less phenolic lignin characterizing angiosperm plants. This is in agreement with the apparent relationship between the number of Polyporales ligninolytic peroxidases with the surface catalytic tryptophan (VPs and LiPs oxidizing nonphenolic lignin) and the frequency of angiosperms as their hosts. Recent character reconstruction based on over 5,000 mushroom-forming species determined that the ancestor of Polyporales had mainly gymnosperms as hosts (31), and during fungal evolution, white-rot fungi specialized in angiosperms, while brown-rot fungi, without ligninolytic peroxidases, became more generalist (14). Our results analyzing ancestral ligninolytic peroxidases and their behavior using real lignin substrates support these conclusions and point to a fascinating coevolution between fungi and plants.

Materials and Methods

The 118 peroxidase sequences were obtained from the genomes of 10 Polyporales (20) and the ascomycete *S. nodorum* sequenced at the Department of Energy's JGI and available from the JGI MycoCosm database (https://mycocosm.jgi.doe.gov/mycocosm/home). PAML 4.7 (32) was used for ancestral sequence reconstruction, using the phylogeny from RAxML (33). PATHd8 (34) was used for time calibration of an ultrametric phylogenetic tree, using the diversification of Pezizomycotina (average 631 Mya), the internal diversification of *Stagonospora nodorum* generic peroxidases (average 403 Mya), and the diversification of the Antrodia clade peroxidases (average 399 Mya) (9) as time constraints.

Four reconstructed ancestral peroxidase sequences and extant PC-LIPA were expressed in *E. coli* and activated in vitro (11). Transient-state kinetic constants were estimated by stopped-flow rapid spectrophotometry (at 25 °C in 0.1 M tartrate, with a pH of 3) using softwood and hardwood lignosulfonates, whose concentrations were referred to the basic phenylpropanoid unit (260 and 290 Da, respectively). Lignosulfonate modification in steady-state treatments (24 h at 25 °C in 50 mM phosphate, with a pH of 5) were analyzed by HSQC 2D NMR after spectral normalization with respect to the δ_H/δ_C 2.49/39.5 ppm signal of the nondeuterated fraction of dimethyl sulfoxide used as NMR solvent. See *SI Appendix* for details. The data supporting the conclusions of this article are included within the article and in the *SI Appendix*.

ACKNOWLEDGMENTS. This work was supported by the EnzOx2 (H2020-BBI-PPP-2015-2-720297, https://www.enzox2.eu) European project and the BIO2017-86559-R and AGL2017-83036-R Spanish projects. The work conducted by JGI was supported by the Office of Science of the US Department of Energy under Contract DE-AC02-05CH11231. We thank Esther Novo-Uzal (Gulbenkian Institute, Oeiras, Portugal) for critical reading of the manuscript and comments on plant and lignin evolution, Guro E. Fredheim (Borregaard AS, Sarpsborg, Norway) for providing the lignosulfonate preparations, José M. Barrasa (University of Alcalá, Spain) for helpful comments on Polyporales ecology and evolution, and Manuel Angulo from the Centro de Investigación Tecnológica e Innovación de la Universidad de Sevilla (CITIUS, Seville, Spain) for the NMR analyses.

1. J. Ralph *et al.*, Lignins: Natural polymers from oxidative coupling of 4-hydroxyphenylpropanoids. *Phytochem. Rev.* **3**, 29–60 (2004).
2. A. T. Martínez, F. J. Ruiz-Dueñas, M. J. Martínez, J. C. Del Río, A. Gutiérrez, Enzymatic delignification of plant cell wall: From nature to mill. *Curr. Opin. Biotechnol.* **20**, 348–357 (2009).
3. T. K. Kirk, R. L. Farrell, Enzymatic "combustion": The microbial degradation of lignin. *Annu. Rev. Microbiol.* **41**, 465–505 (1987).
4. A. T. Martínez, S. Camarero, F. J. Ruiz-Dueñas, M. J. Martínez, "Biological lignin degradation" in *Lignin Valorization: Emerging Approaches*, G. T. Beckham, Ed. (RSC, Cambridge, UK, 2018), chap. 8, pp. 199–225.
5. E. Fernández-Fueyo *et al.*, Structural implications of the C-terminal tail in the catalytic and stability properties of manganese peroxidases from ligninolytic fungi. *Acta Crystallogr. D Biol. Crystallogr.* **70**, 3253–3265 (2014).
6. T. Mester *et al.*, Oxidation of a tetrameric nonphenolic lignin model compound by lignin peroxidase. *J. Biol. Chem.* **276**, 22985–22990 (2001).
7. F. J. Ruiz-Dueñas *et al.*, Substrate oxidation sites in versatile peroxidase and other basidiomycete peroxidases. *J. Exp. Bot.* **60**, 441–452 (2009).
8. V. Sáez-Jiménez *et al.*, Role of surface tryptophan for peroxidase oxidation of nonphenolic lignin. *Biotechnol. Biofuels* **9**, 198 (2016).
9. D. Floudas *et al.*, The Paleozoic origin of enzymatic lignin decomposition reconstructed from 31 fungal genomes. *Science* **336**, 1715–1719 (2012).
10. D. Hibbett, R. Blanchette, P. Kenrick, B. Mills, Climate, decay, and the death of the coal forests. *Curr. Biol.* **26**, R563–R567 (2016).
11. I. Ayuso-Fernández, A. T. Martínez, F. J. Ruiz-Dueñas, Experimental recreation of the evolution of lignin-degrading enzymes from the Jurassic to date. *Biotechnol. Biofuels* **10**, 67 (2017).
12. I. Ayuso-Fernández, F. J. Ruiz-Dueñas, A. T. Martínez, Evolutionary convergence in lignin-degrading enzymes. *Proc. Natl. Acad. Sci. U.S.A.* **115**, 6428–6433 (2018).
13. I. Ayuso-Fernández, A. L. De Lacey, F. J. Cañada, F. J. Ruiz-Dueñas, A. T. Martínez, Redox potential increased during the evolution of enzymes degrading recalcitrant lignin. *Chemistry* **25**, 2708–2712 (2018).
14. F. S. Krah *et al.*, Evolutionary dynamics of host specialization in wood-decay fungi. *BMC Evol. Biol.* **18**, 119 (2018).
15. K. V. Sarkanen, H. L. Hergert, "Classification and distribution" in *Lignins: Occurrence, Formation, Structure and Reactions*, K. V. Sarkanen, C. H. Ludwig, Eds. (Wiley-Interscience, New York, NY, 1971), pp. 43–94.
16. L. Li *et al.*, The last step of syringyl monolignol biosynthesis in angiosperms is regulated by a novel gene encoding sinapyl alcohol dehydrogenase. *Plant Cell* **13**, 1567–1586 (2001).
17. B. Menden, M. Kohlhoff, B. M. Moerschbacher, Wheat cells accumulate a syringyl-rich lignin during the hypersensitive resistance response. *Phytochemistry* **68**, 513–520 (2007).
18. V. Sáez-Jiménez *et al.*, Demonstration of lignin-to-peroxidase direct electron transfer: A transient-state kinetics, directed mutagenesis, EPR and NMR study. *J. Biol. Chem.* **290**, 23201–23213 (2015).
19. H. Sixta, A. Potthast, A. W. Krotschek, "Chemical pulping processes" in *Handbook of Pulping*, H. Sixta, Ed. (Wiley, Weinheim, Germany, 2006), pp. 109–509.
20. F. J. Ruiz-Dueñas *et al.*, Lignin-degrading peroxidases in Polyporales: An evolutionary survey based on 10 sequenced genomes. *Mycologia* **105**, 1428–1444 (2013).
21. D. Martinez *et al.*, Genome sequence of the lignocellulose degrading fungus *Phanerochaete chrysosporium* strain RP78. *Nat. Biotechnol.* **22**, 695–700 (2004).
22. L. G. Nagy *et al.*, Comparative genomics of early-diverging mushroom-forming fungi provides insights into the origins of lignocellulose decay capabilities. *Mol. Biol. Evol.* **33**, 959–970 (2016).
23. R. Riley *et al.*, Extensive sampling of basidiomycete genomes demonstrates inadequacy of the white-rot/brown-rot paradigm for wood decay fungi. *Proc. Natl. Acad. Sci. U.S.A.* **111**, 9923–9928 (2014).
24. J. Ralph, L. L. Landucci, "NMR of lignin" in *Lignin and Lignans: Advances in Chemistry*, C. Heitner, D. Dimmel, J. Schmidt, Eds. (CRC Press, Boca Raton, FL, 2010), pp. 137–243.
25. J. L. Morris *et al.*, The timescale of early land plant evolution. *Proc. Natl. Acad. Sci. U.S.A.* **115**, E2274–E2283 (2018).
26. J. K. Weng, C. Chapple, The origin and evolution of lignin biosynthesis. *New Phytol.* **187**, 273–285 (2010).
27. J. K. Weng, T. Akiyama, J. Ralph, C. Chapple, Independent recruitment of an O-methyltransferase for syringyl lignin biosynthesis in *Selaginella moellendorffii*. *Plant Cell* **23**, 2708–2724 (2011).
28. E. Novo-Uzal, F. Pomar, L. V. G. Ros, J. M. Espineira, A. R. Barcelo, "Evolutionary history of lignins" in *Lignins: Biosynthesis, Biodegradation and Bioengineering*, L. Jouanin, C. Lapierre, Eds. (Advances in Botanical Research, Academic Press, London, 2012), vol. 61, pp. 311–350.
29. Y. Z. Lai, X. P. Guo, Variation of the phenolic hydroxyl group content in wood lignins. *Wood Sci. Technol.* **25**, 467–472 (1991).
30. S. Camarero, P. Bocchini, G. C. Galletti, A. T. Martínez, Pyrolysis-gas chromatography/mass spectrometry analysis of phenolic and etherified units in natural and industrial lignins. *Rapid Commun. Mass Spectrom.* **13**, 630–636 (1999).
31. T. Varga *et al.*, Megaphylogeny resolves global patterns of mushroom evolution. *Nat. Ecol. Evol.* **3**, 668–678 (2019).
32. Z. Yang, PAML 4: Phylogenetic analysis by maximum likelihood. *Mol. Biol. Evol.* **24**, 1586–1591 (2007).
33. A. Stamatakis, P. Hoover, J. Rougemont, A rapid bootstrap algorithm for the RAxML Web servers. *Syst. Biol.* **57**, 758–771 (2008).
34. T. Britton, C. L. Anderson, D. Jacquet, S. Lundqvist, K. Bremer, Estimating divergence times in large phylogenetic trees. *Syst. Biol.* **56**, 741–752 (2007).